Solid State Phenomena *Submitted: 2021-10-27*
ISSN: 1662-9779, Vol. 333, pp 219-225 *Revised: 2021-11-25*
doi:10.4028/p-76scj1 *Accepted: 2021-11-25*
Online: 2022-06-10

A Node-Based Strain Smoothing Technique for Free Vibration Analysis of Textile-Like Sheet Materials

Nguyễn T. Quyền[1,a*], Nguyễn T. Quốc[2,3,b], Nguyễn Đ. Trụ[4,c], Abel J.P. Gomes[2,3,d] and Fernando B.N. Ferreira[1,e]

[1]2C2T - Centro de Ciência e Tecnologia Têxtil, Departamento de Engenharia Têxtil, Universidade do Minho, Campus de Azurém, 4804-533 Guimarães, Portugal

[2]Departamento de Informática, Universidade da Beira Interior, Convento de Sto. António, 6201-001 Covilhã, Portugal

[3]Instituto de Telecomunicações, Rua Marquês d'Ávila e Bolama, 6201-001 Covilhã, Portugal

[4]Faculty of Textile and Garment Technology, Ho Chi Minh City Industry and Trade College, 20 Tang Nhon Phu, Phuoc Long B Ward, District 9, Ho Chi Minh, Vietnam

[a]quyen@2c2t.uminho.pt, [b]quochcmvn@gmail.com, [c]dinhtru1509@gmail.com, [d]agomes@di.ubi.pt, [e]fnunes@det.uminho.pt,

Keywords: Textile-like sheet material; Mindlin–Reissner plate theory; Free vibration analysis; Finite element method; Strain smoothing technique; Node-based smoothed finite element

Abstract. This paper presents an implementation of the node-based smoothed finite element method and Reissner-Mindlin plate theory for a four node isoparametric shell element to improve the numerical precision and computational efficiency subjected to free vibration analysis of textile-like sheet materials. A one smoothing cell integration scheme in the strain smoothing technique is implemented to contrast the shear locking phenomenon that may exists in the analysis for moderately-thick and thick shell models. Various numerical results of free vibration analysis for a multi-layer nonwoven fabric sample are compared with other existing analytical solutions and numerical solutions in literatures to demonstrate the effectiveness of the present method. An advantage of the present formulation is that it can improve the numerical precision without decreasing the computational efficiency.

Introduction

The finite element method (FEM) is an efficient tool for analyses of shell/plate structures to help understanding of vibration and buckling behavior of textile-like sheet materials, e.g., the basic practical problem of residual curvature in the fusible interlinings [1-3], through garment manufacturing and also during its use as a garment, as detailed in references [4-6]. However, FEM has some limitations or drawbacks being found during its intensive applications, including in references [7-10]. The node-based smoothed finite element method (NS-FEM), presented by Liu and his coworkers [11-14], is a method formulated through the combinations of the conventional FEM and some techniques from the meshfree methods, and have partly resolved some known issues existing in standard FEM. The strain smoothing stabilization technique evaluates the nodal strain as the divergence of a spatial average of the compatible strain field avoiding the derivative evaluations of mesh-free shape functions at nodes and hence eliminates defective modes [10, 15, 16]. This technique avoids evaluating derivatives of mesh-free shape functions at nodes and therefore eliminates defective modes. This paper is to present a finite element formulation of plate/shell structures based on the node-based strain smoothing technique in finite elements and Mindlin-Reissner plate theory. The present method illustrates that the numerical solution can help increasing the numerical accuracy and the computational efficiency for free vibration analysis of textile-like sheet materials.

Finite Element Formulation

Assume that a fabric sheet is a three-dimensional elastic domain $\Omega \in \mathbb{R}^3$ as a solid body being thin in thickness but having significant length in other two directions [17, 18]. The domain Ω has a Lipschitz-continuous boundary Γ and a body force b. The first parts of boundary Γ, namely Γ_u where Dirichlet conditions $\bar{\mathrm{u}}$ are prescribed, and the second part denoted with Γ_t where Neumann conditions $\mathrm{t} = \bar{\mathrm{t}}$ are also prescribed. Γ_u and Γ_t construct a partition of the boundary Γ for instance $\Gamma = \Gamma_u \cup \Gamma_t$.

The static equilibrium equation governing the solid can be written in term of the stress field as

$$\mathbf{L}^{\mathrm{T}}\boldsymbol{\sigma} + \mathbf{b} = \mathbf{0} \text{ in } \Omega. \tag{1}$$

Let $\mathbf{D}$ be the elasticity matrix [18, 19] that governs the material constants of the solid for plane stress analysis [13, 18, 20, 21] in the present formulation. The stresses $\boldsymbol{\sigma}$ relate to the strains $\boldsymbol{\varepsilon}$ via the generalized Hook's law (also known as the constitutive equations), which gives

$$\boldsymbol{\sigma} = \mathbf{D}\boldsymbol{\varepsilon}. \tag{2}$$

The strain matrix $\boldsymbol{\varepsilon}$ relates to the displacements in the form of compatibility equations (or the kinematic equations)

$$\boldsymbol{\varepsilon} = \mathbf{L}\mathbf{u}, \tag{3}$$

with $\mathbf{u}$ is the displacement component at a point in Ω. Substituting Eq. 8 into Eq. 7 which gives the equilibrium equation in terms of the displacements.

The conditions of Dirichlet boundary Γ_u and the Neumann boundary Γ_t are also defined as

$$\mathbf{u} = \mathbf{u}_{\Gamma}, \tag{4}$$

$$\mathbf{L}_n^{\mathrm{T}}\boldsymbol{\sigma} = \mathbf{t}_{\Gamma}, \tag{5}$$

in which $\mathbf{L}_n$ is the matrix of unit outward normal components. Hence, the strain energy (or potential energy) for elastic solid can be quantified via

$$\mathbf{U} = \frac{1}{2}\int_{\Omega} \boldsymbol{\varepsilon}^T(\mathbf{x})\boldsymbol{\sigma}(\mathbf{x})\, d\Omega = \frac{1}{2}\int_{\Omega} \boldsymbol{\varepsilon}^T(\mathbf{x})\mathbf{c}\boldsymbol{\varepsilon}(\mathbf{x})\, d\Omega. \tag{6}$$

The configuration domain $\Omega \in \mathbb{R}^3$ that forms the shell mid-surface based on the Mindlin-Reissner plate theory being defined by

$$V = \left\{(x,y,z) \in \mathbb{R}^3 | (x,y) \in \Omega \subset \mathbb{R}^2, z \in \left[-\frac{t}{2}, \frac{t}{2}\right]\right\}. \tag{7}$$

For approximation of the stress state in a moderately thick shell, to which the analysis of the membrane deformations can be performed, the displacement assumption gives

$$\begin{aligned} u(x,y,z) &= u_0(x,y) + z\beta_x(x,y) \\ v(x,y,z) &= v_0(x,y) + z\beta_y(x,y). \\ w(x,y,z) &= w_0(x,y) \end{aligned} \tag{8}$$

in which u_0, v_0 and w_0 denote the displacement components along x-, y- and z-directions, respectively. β_x and β_y stand for the normal rotations to the undeformed mid-surface corresponding to the x-z and y-z planes having $\beta_x = \frac{\partial \mathrm{w}}{\partial x}$ and $\beta_y = \frac{\partial \mathrm{w}}{\partial y}$.

The membrane strain $\boldsymbol{\varepsilon}^m$, curvature strain $\boldsymbol{\varepsilon}^b$ are calculated from the corresponding 2D differential operators $\mathbf{L}$, as presented in Eq. 8, which are

$$\boldsymbol{L}_{2D}^m = \begin{bmatrix} \frac{\partial}{\partial x} & 0 \\ 0 & \frac{\partial}{\partial y} \\ \frac{\partial}{\partial y} & \frac{\partial}{\partial x} \end{bmatrix} \text{ and } \mathbf{L}_{2D}^b = \begin{bmatrix} 0 & \frac{\partial}{\partial x} \\ -\frac{\partial}{\partial y} & 0 \\ \frac{-\partial}{\partial x} & \frac{\partial}{\partial y} \end{bmatrix}. \tag{9}$$

From the displacement components in Eq. 8 with $\mathbf{u} = [u_0 \quad v_0 \quad w_0]^T$ and $\boldsymbol{\beta} = [\beta_x \quad \beta_y]^T$, Eq. 9 can be rewritten as

$$\boldsymbol{\varepsilon}^m = \boldsymbol{L}_{2D}^m \boldsymbol{u} = \begin{bmatrix} u_{0,x} \\ v_{0,y} \\ u_{0,y} + v_{0,x} \end{bmatrix}, \boldsymbol{\varepsilon}^b = \boldsymbol{L}_{2D}^b \boldsymbol{\beta} = \begin{bmatrix} \beta_{x,x} \\ -\beta_{y,y} \\ \beta_{x,y} - \beta_{y,x} \end{bmatrix}, \tag{10}$$

while the transverse shear strain $\boldsymbol{\varepsilon}^s$ can be quantified using

$$\boldsymbol{\varepsilon}^s = \begin{Bmatrix} \gamma_{xy} \\ \gamma_{yz} \end{Bmatrix} = \begin{bmatrix} w_{,x} + \beta_x \\ w_{,y} - \beta_y \end{bmatrix}. \tag{11}$$

Let the problem domain $\Omega \in \mathbb{R}^3$ be discretized into a set of N_e four-node isoparametric quadrilateral shell elements Ω^e referred to as Q4 with boundary Γ^e and the total number of nodes N_I. Let $\mathrm{N}_I(\mathbf{x})$ and $\mathbf{d}_I = [u_I \quad v_I \quad w_I \quad \theta_{xI} \quad \theta_{yI}]^T$, respectively, indicate the bilinear shape functions and the vector of nodal degrees of freedom associated with node I. The displacement assumption [22] and strains in Eq. 13 and Eq. 15 within any element Ω^e can be written as

$$\boldsymbol{u}^h = \sum_{I=1}^{n_I} \begin{bmatrix} \mathrm{N}_I(\mathbf{x}) & 0 & 0 & 0 & 0 \\ 0 & \mathrm{N}_I(\mathbf{x}) & 0 & 0 & 0 \\ 0 & 0 & \mathrm{N}_I(\mathbf{x}) & 0 & 0 \\ 0 & 0 & 0 & 0 & \mathrm{N}_I(\mathbf{x}) \\ 0 & 0 & 0 & \mathrm{N}_I(\mathbf{x}) & 0 \end{bmatrix} \mathbf{d}_I, \tag{12}$$

$$\boldsymbol{\varepsilon}^m = \sum_I \mathbf{B}_I^m \mathbf{d}_I, \boldsymbol{\varepsilon}^b = \sum_I \mathbf{B}_I^b \mathbf{d}_I, \boldsymbol{\varepsilon}^s = \sum_I \mathbf{B}_I^s \mathbf{d}_I, \tag{13}$$

$$\mathbf{B}_I^m = \begin{bmatrix} \mathrm{N}_{I,x} & 0 & 0 & 0 & 0 \\ 0 & \mathrm{N}_{I,y} & 0 & 0 & 0 \\ \mathrm{N}_{I,y} & \mathrm{N}_{I,x} & 0 & 0 & 0 \end{bmatrix}, \tag{14}$$

$$\mathbf{B}_I^b = \begin{bmatrix} 0 & 0 & 0 & \mathrm{N}_{I,x} & 0 \\ 0 & 0 & -\mathrm{N}_{I,y} & 0 & 0 \\ 0 & 0 & -\mathrm{N}_{I,x} & \mathrm{N}_{I,y} & 0 \end{bmatrix}, \tag{15}$$

$$\mathbf{B}_I^s = \begin{bmatrix} 0 & 0 & \mathrm{N}_{I,x} & 0 & \mathrm{N}_I \\ 0 & 0 & \mathrm{N}_{I,y} & -\mathrm{N}_I & 0 \end{bmatrix}. \tag{16}$$

In the free analysis, the formulation of a Mindlin-Reissner shell can be written in the matrix form,

$$\mathbf{m}^e \ddot{\mathbf{d}} + \mathbf{k}^e \mathbf{d} = \mathbf{0}, \tag{17}$$

where the element stiffness matrix $\mathbf{k}^e$ and element mass matrix $\mathbf{m}^e$ are given as

$$\mathbf{k}^e = \int_{\Omega^e} (\mathbf{B}^m)^T \mathbf{D}^m \mathbf{B}^m \mathrm{d}\Omega + \int_{\Omega^e} (\mathbf{B}^b)^T \mathbf{D}^b \mathbf{B}^b \mathrm{d}\Omega + \int_{\Omega^e} (\mathbf{B}^s)^T \mathbf{D}^s \mathbf{B}^s \mathrm{d}\Omega, \tag{18}$$

$$\mathbf{m}^e = \int_{\Omega^e} \mathbf{N}^T \mathbf{m} \mathbf{N} \mathrm{d}\Omega, \mathbf{m} = \rho \begin{bmatrix} t & 0 & 0 & 0 & 0 & 0 \\ 0 & t & 0 & 0 & 0 & 0 \\ 0 & 0 & t & 0 & 0 & 0 \\ 0 & 0 & 0 & 0 & \frac{t^3}{12} & 0 \\ 0 & 0 & 0 & \frac{t^3}{12} & 0 & 0 \\ 0 & 0 & 0 & 0 & 0 & 0 \end{bmatrix}, \tag{19}$$

with ρ being the density of the fabric sheet.

The stiffness co-efficient of the drilling degrees of freedom θ_{zI} associated with each node $I \in \Omega^e$, as figured out in the literatures [21, 23], is set to be

$$\theta_{zI} = 10^{-3} \times max\{\text{diag}(\mathbf{k}_I^e)\}, \tag{20}$$

the element stiffness matrix related to node I is, therefore, written as

$$\mathbf{k}_I^e = \begin{bmatrix} \mathbf{k}_{I\ 2x2}^m & \mathbf{0}_{2\times3} & 0 \\ \mathbf{0}_{3\times2} & \mathbf{k}_I^b + \mathbf{k}_I^s & 0 \\ \mathbf{0}_{1\times2} & \mathbf{0}_{1\times3} & \theta_{zI} \end{bmatrix}. \tag{21}$$

The shear locking phenomenon may exist in moderately thick shell models as figured out in works [21, 23-26]. In the present formulation, the shear strain term is evaluated using one smoothing cell integration scheme (see Eq. 24) in the strain smoothing technique to overcome the shear locking problem.

Consider the node-based strain smoothing technique, each of element $\Omega^e \in \Omega$ is further subdivided into 4 triangular elements, in which the centroid node of Ω^e is the first node of each sub triangular element, with $\Omega^e = \bigcup_{k=1}^4 \Omega_k^s$, $\Omega_i^s \cap \Omega_j^s = \emptyset, i \neq j \ (i = 1, \dots, 4; j = 1, \dots, 4)$, and Ω_k^s indicates the kth smoothing domain of the element Ω^e. Each smoothing domain has the total number n_b^s of boundary segments that $\Gamma_k^s = \bigcup_{b=1}^{n_b^s} \Gamma_{kb}^e$ with $\Gamma_i^s \cap \Gamma_j^s = \emptyset, i \neq j \ (i = 1, \dots, n_b^s; j = 1, \dots, n_b^s)$. The total number of smoothing domains within each discretized element Ω^e can be equal to the total number of discretized elements Ω^e within the system domain Ω. This means that one discretized element Ω^e can be used as one smoothing domain Ω_k^s. Now, direct apply strain smoothing technique with linear strain fields for static as in works [9, 27, 28] to Eq. 13 which can be approximated as

$$\boldsymbol{\varepsilon}^m(\mathbf{x}_k) = \frac{1}{A_k^s}\int_{\Gamma_k^s} \boldsymbol{n}.\boldsymbol{u}(\mathbf{x}_k)\, d\Gamma = \frac{1}{A_k^s}\sum_{I=1}^3 \begin{bmatrix} \bar{b}_{kIx} & 0 & 0 & 0 & 0 & 0 \\ 0 & \bar{b}_{kIy} & 0 & 0 & 0 & 0 \\ \bar{b}_{kIy} & \bar{b}_{kIx} & 0 & 0 & 0 & 0 \end{bmatrix}.\boldsymbol{d}_I, \tag{22}$$

$$\boldsymbol{\varepsilon}^b(\mathbf{x}_k) = \frac{1}{A_k^s}\int_{\Gamma_k^s} \boldsymbol{n}.\boldsymbol{u}(\mathbf{x}_k)\, d\Gamma = \frac{1}{A_k^s}\sum_{I=1}^3 \begin{bmatrix} 0 & 0 & \bar{b}_{kIx} & 0 & 0 & 0 \\ 0 & -\bar{b}_{kIy} & 0 & 0 & 0 & 0 \\ 0 & -\bar{b}_{kIx} & \bar{b}_{kIy} & 0 & 0 & 0 \end{bmatrix}.\boldsymbol{d}_I, \tag{23}$$

$$\boldsymbol{\varepsilon}^s(\mathbf{x}) = \frac{1}{A^e}\int_{\Gamma^e} \boldsymbol{n}.\boldsymbol{u}(\mathbf{x})\, d\Gamma = \frac{1}{A^e}\sum_{I=1}^4 \begin{bmatrix} 0 & 0 & \bar{b}_{kIx} & 0 & \bar{b}_{kI} \\ 0 & 0 & \bar{b}_{kIy} & -\bar{b}_{kI} & 0 \end{bmatrix}.\boldsymbol{d}_I, \tag{24}$$

with

$$\bar{b}_{kIx} = \frac{1}{A_k^s}\int_{\Gamma_k^s} n_x N_I\, d\Gamma = \frac{1}{A_k^s}\sum_{b=1}^{n_b^s} n_{xb}.N_I(\mathrm{x}_b^G).\, l_b, \tag{25}$$

$$\bar{b}_{kIy} = \frac{1}{A_k^s}\int_{\Gamma_{k,c}^e} n_y N_I\, d\Gamma = \frac{1}{A_k^s}\sum_{b=1}^{n_b^s} n_{yb}.N_I(\mathrm{x}_b^G).\, l_b. \tag{26}$$

In Eqs. 22, 23 and 24, $A^e = \int_{\Omega^e} d\Omega$ is the area of Ω^e, while $A_k^s = \int_{\Omega_k^s} d\Omega$ is the area of the kth smoothing domain $\Omega_k^s \subset \Omega^e$. In Eq. 25 and Eq. 26, n_{xb} and n_{yb} indicate the components of the outward unit normal to the bth boundary segment and x_b^G is the coordinate value of Gauss point of the bth boundary segment.

For analyzing the free vibration effect, the discretized governing equation in terms of the global stiffness matrices **K** and the global mass matrix **M** regarding to Eq. 18 and Eq 19, which given

$$\mathbf{M}\ddot{\boldsymbol{d}} - \mathbf{K}\boldsymbol{d} = \mathbf{0}. \tag{27}$$

Substitute the general solution $\boldsymbol{d} = \bar{\boldsymbol{d}}\exp(i\omega t)$ into Eq. 27, the natural frequency ω can be quantified by solving

$$(\mathbf{K} - \omega^2\mathbf{M})\bar{\boldsymbol{d}} = \mathbf{0}. \tag{28}$$

Numerical Example and Results

In present study, a numerical example for a linear static free vibration analysis of multi-layer nonwoven fabric sheet, a wide range of the sub-cell $\Omega_c^s \subset \Omega^e$ is considered, together with the simply supported boundary conditions. The non-dimensional natural frequencies ϖ for a non-woven fabric sheet having the thickness-to-length ratio $\frac{t}{L}$, the shear factor corrections k and the Poisson's ratio ν are shown in Fig. 1.

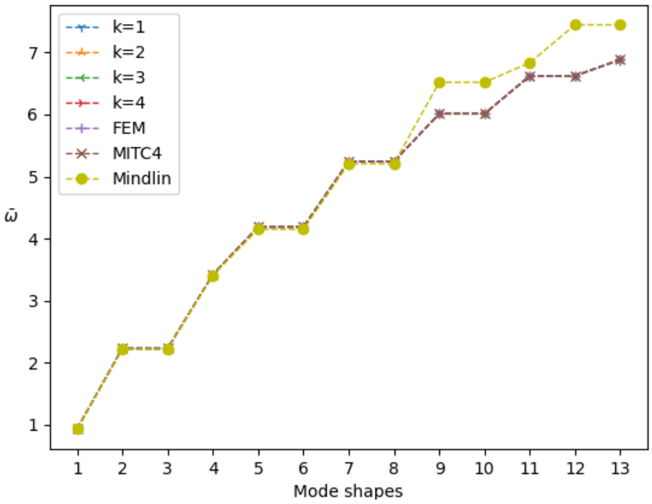

Figure 1. Mode shapes of non-dimensional natural frequency ϖ for a square simply supported non-woven fabric sheet with $\frac{t}{L} = 0.1$, $k = 0.8333$, $\nu = 0.3$ and $35 \times 35\ \Omega^e$.

The numerical results of linear static and free vibration analysis, as illustrated in Fig. 1, indicate a good agreement to the to the analytical solution (Mindlin's theory) [29], and numerical solutions based on MITC4 and conventional FEM under the simply supported boundary conditions.

Conclusion

The present method can reduce the practical implementation effort and computational cost in comparison to the standard FEM approaches. The shear locking problem has been resolved via the implementation using one smoothing cell integration in the strain smoothing technique. The numerical results show that the solutions can improve numerical accuracy and computational efficiency subjected to free vibration analysis of textile-like sheet materials.

Acknowledgment

The first and fourth author acknowledge FCT for the conceded financial support through Project UID/CTM/00264/2019 of 2C2T – Centro de Ciência e Tecnologia Têxtil, hold by National Founds of FCT/MCTES. The second and third author acknowledge support by FCT/MCTES through national funds and when applicable co-funded EU funds under the project SFRH/BD/136554/2018.

References

[1] Zhang, Q. and C.-W. Kan, A Review of Fusible Interlinings Usage in Garment Manufacture, *Polymers,* 10 (2018), doi:10.3390/polym10111230

[2] Phebe, K., K. Kaliappa, and B. Chandrasekaran, Evaluating performance characteristics of different fusible intertinings, *Indian Journal of Fibre and Textile Research,* 39 (2014) 380-385,

[3] Lai, S.S., Optimal combinations of face and fusible interlining fabrics, *International Journal of Clothing Science and Technology,* 13 (2001) 322-338, doi:10.1108/09556220110405073

[4] Behera, B.K. and P.K. Hari, Woven Textile Structure: Theory And Applications, Elsevier Science, 2010.

[5] Namdar, Ö. and H. Darendeliler, Buckling, postbuckling and progressive failure analyses of composite laminated plates under compressive loading, Composites Part B: Engineering, 120 (2017) 143-151, doi:https://doi.org/10.1016/j.compositesb.2017.03.066

[6] Rajesh, M. and J. Pitchaimani, Experimental investigation on buckling and free vibration behavior of woven natural fiber fabric composite under axial compression, Composite Structures, 163 (2017) 302-311, doi:https://doi.org/10.1016/j.compstruct.2016.12.046

[7] Hughes, T.J.R., The Finite Element Method: Linear Static and Dynamic Finite Element Analysis, Dover Publications, 2012.

[8] Belytschko, T., W.K. Liu, B. Moran, and K. Elkhodary, Nonlinear Finite Elements for Continua and Structures, Wiley, 2013.

[9] Zeng, W. and G.R. Liu, Smoothed Finite Element Methods (S-FEM): An Overview and Recent Developments, Archives of Computational Methods in Engineering, 25 (2018) 397-435, doi:10.1007/s11831-016-9202-3

[10] Liu, G.R., An Overview on Meshfree Methods: For Computational Solid Mechanics, International Journal of Computational Methods, 13 (2016) 1630001, doi:10.1142/S0219876216300014

[11] Liu, G.R., K.Y. Dai, and T.T. Nguyen, A Smoothed Finite Element Method for Mechanics Problems, Computational Mechanics, 39 (2007) 859-877, doi:10.1007/s00466-006-0075-4

[12] Nguyen-Xuan, H., T. Rabczuk, N. Nguyen-Thanh, T. Nguyen-Thoi, and S. Bordas, A node-based smoothed finite element method with stabilized discrete shear gap technique for analysis of Reissner–Mindlin plates, Computational Mechanics, 46 (2010) 679-701, doi:10.1007/s00466-010-0509-x

[13] Thai-Hoang, C., N. Nguyen-Thanh, H. Nguyen-Xuan, T. Rabczuk, and S. Bordas, A cell — based smoothed finite element method for free vibration and buckling analysis of shells, KSCE Journal of Civil Engineering, 15 (2011) 347-361, doi:10.1007/s12205-011-1092-1

[14] Liu, G.-R. and T. Nguyen-Thoi, Smoothed finite element methods, Taylor and Francis Group, LLC, 2010.

[15] Liu, G., K. Dai, and T. Nguyen, A Smoothed Finite Element Method for Mechanics Problems, Computational Mechanics, 39 (2007) 859-877, doi:10.1007/s00466-006-0075-4

[16] Liu, G.R., T.T. Nguyen, K.Y. Dai, and K.Y. Lam, Theoretical aspects of the smoothed finite element method (SFEM), International Journal for Numerical Methods in Engineering, 71 (2007) 902-930, doi:10.1002/nme.1968

[17] Zulifqar, A., Z. Khaliq, and H. Hu, Textile Mechanics, in: In Handbook of Fibrous Materials, 2020, pp. 455-476)

[18] Hu, J., Structure and mechanics of woven fabrics, Woodhead Publishing Ltd., Cambridge, 2004.

[19] Veit, D., Simulation in textile technology: Theory and applications (1 ed.), Woodhead Publishing, 2012.

[20] Gigli, N. and B. Han, Sobolev Spaces on Warped Products, Journal of Functional Analysis (2015), doi:10.1016/j.jfa.2018.03.021

[21] Zienkiewicz, O.C. and R.L. Taylor, The Finite Element Method for Solid and Structural Mechanics (6 ed. Vol. 2), Butterworth-Heinemann Ltd, 2005.

[22] Hinton, E., Numerical methods and software for dynamic analysis of plates and shells, Pineridge Press, Swansea, U.K., 1988.

[23] Zienkiewicz, O.C., R.L. Taylor, and J.Z. Zhu, Shells as an assembly of flat elements, in: In The Finite Element Method Set (Sixth Edition), Oxford, Butterworth-Heinemann, 2005, pp. 426-453)

[24] Hughes, T.J.R., M. Cohen, and M. Haroun, Reduced and selective integration techniques in the finite element analysis of plates, Nuclear Engineering and Design, 46 (1978) 203-222, doi:10.1016/0029-5493(78)90184-x

[25] Malkus, D.S. and T.J.R. Hughes, Mixed finite element methods reduced and selective integration techniques: a unification of concepts, Computer Methods in Applied Mechanics and Engineering, 15 (1978) 63-81,

[26] Bathe, K.-J. and E.N. Dvorkin, A formulation of general shell elements—the use of mixed interpolation of tensorial components, International Journal for Numerical Methods in Engineering, 22 (1986) 697-722, doi:10.1002/nme.1620220312

[27] Liu, G.-R., The smoothed finite element method (S-FEM): A framework for the design of numerical models for desired solutions, Frontiers of Structural and Civil Engineering, 13 (2019) 456-477, doi:10.1007/s11709-019-0519-5

[28] Yue, J., G.-R. Liu, M. Li, and R. Niu, A cell-based smoothed finite element method for multi-body contact analysis using linear complementarity formulation, International Journal of Solids and Structures (2018), doi:https://doi.org/10.1016/j.ijsolstr.2018.02.016

[29] Liew, K.M., J. Wang, T.Y. Ng, and M.J. Tan, Free vibration and buckling analyses of shear-deformable plates based on FSDT meshfree method, Journal of Sound and Vibration, 276 (2004) 997-1017, doi:https://doi.org/10.1016/j.jsv.2003.08.026